SUPPLEMENTARY TABLES

Table S1. Crystallographic data collection and refinement statistics for wild-type Ago (4A5 bulge) or D546N catalytic mutant Ago (7T8 and 5A6 bulges) ternary complex containing bulges on guide strand.

	7T8 Bulge	4A5 Bulge	5A6 Bulge
Data collection			
Space group	$P2_12_12_1$	$P4_132$	$P2_13$
Cell dimensions			
a, *b*, *c* (Å)	112.7, 115.0, 160.4	202.1, 202.1, 202.1	201.8, 201.8, 201.8
α, β, γ (°)	90, 90, 90	90, 90, 90	90, 90, 90
Resolution (Å)	50-2.63 (2.72-2.63)	50-3.1 (3.15-3.1)	50-3.3 (3.4-3.3)
R_{sym} or R_{merge}	0.1 (0.57)	0.17 (0.80)	0.106 (0.908)
$I/\sigma I$	17.7 (2.0)	9.7 (1.5)	45.5 (4.2)
Completeness (%)	97.5 (95.3)	98.9 (99.4)	100 (100)
Redundancy	4.9 (3.3)	6.6 (5.7)	33.8 (26.4)
Refinement			
Resolution (Å)	50-2.63	50-3.1	50-3.3
No. reflections	60,976	25,862	37,315
$R_{work/}$ R_{free}	24.9/28.2	21.4/27.5	25.2/29.4
No. atoms			
Protein	8,818	5,098	10,369
Ligand/ion	1,267	718	1,470
Water	21		3
B-factors			
Protein	75.4	57.4	58.4
Ligand/ion	87.9	68.4	49.2
Water	55.4		24.2
R.m.s deviations			
Bond lengths (Å)	0.010	0.011	0.013
Bond angles (°)	1.056	1.633	1.703

*Highest resolution shell is shown in parenthesis.

Table S2. Crystallographic data collection and refinement statistics for D546N catalytic mutant Ago ternary complex containing bulges on target strand.

	6'U7' Bulge	6'A7' Bulge	9'U10' Bulge
Data collection			
Space group	$P4_132$	$P4_132$	$P4_32_12$
Cell dimensions			
a, *b*, *c* (Å)	202.4, 202.4, 202.4	200.8, 200.8, 200.8	109.1,109.1, 184.6
α, β, γ (°)	90, 90, 90	90, 90, 90	90, 90, 90
Resolution (Å)	50-2.8 (2.9-2.8)	50-2.9 (2.95-2.9)	50-2.9 (2.95-2.9)
R_{sym} or R_{merge}	0.086 (0.388)	0.1 (0.528)	0.05 (0.512)
$I/\sigma I$	18.8 (2.2)	15.8 (2.0)	46.5 (2.9)
Completeness (%)	99.5 (98.3)	99.3 (99.0)	99.8 (99.8)
Redundancy	8.7 (4.8)	8.8 (5.9)	9.9 (7.7)
Refinement			
Resolution (Å)	50-2.8	50-2.9	50-2.9
No. reflections	35,178	29,402	25,323
$R_{work/}$ R_{free}	20.5/24.9	21.4/25.7	21.5/28.1
No. atoms			
Protein	5,237	5,241	5,145
Ligand/ion	785	799	817
Water	24		
B-factors			
Protein	58.4	79.8	92.6
Ligand/ion	58.2	74.3	143.3
Water	42.9		
R.m.s deviations			
Bond lengths (Å)	0.011	0.009	0.006
Bond angles (º)	1.527	1.299	0.979

*Highest resolution shell is shown in parenthesis.

SUPPLEMENTARY FIGURES

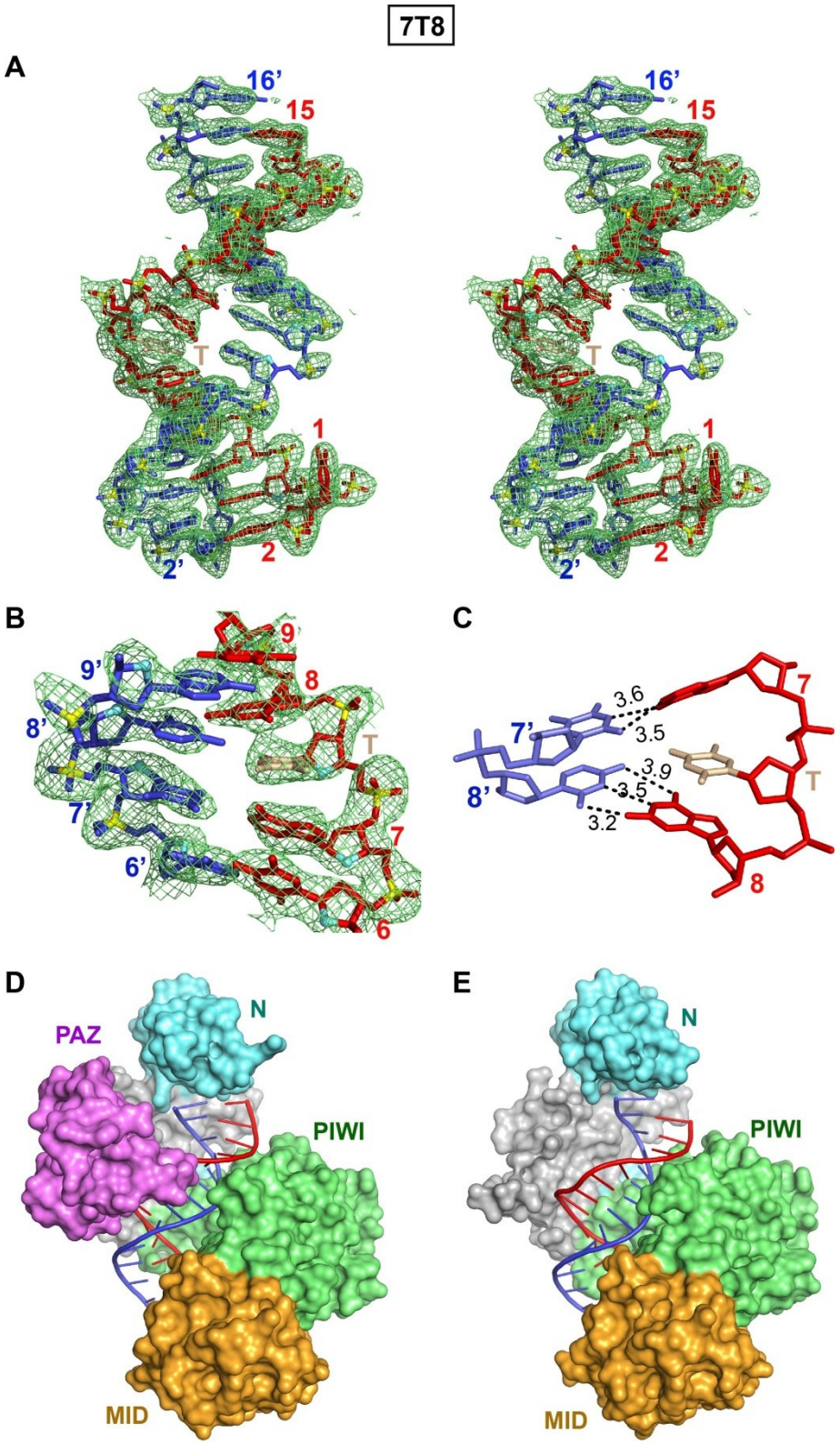

Figure S1. Details of the Stacked-in Thymine in the *Tt*Ago (D546N Catalytic Mutant) Ternary Complex Containing a 7T8 Bulge Within the Seed Segment of the DNA Guide Strand.

(A) Stereo view of the 2Fo-Fc electron density maps (1σ) for the entire guide and target strands of the 7T8 bulge on the guide strand of the *Tt*Ago ternary complex.

(B) 2Fo-Fc electron density maps (1σ) for the guide (nts 6-9) and target (nts 6'-9') strands of the 7T8 bulge on the guide strand of the *Tt*Ago ternary complex. The stacked- in T of the 7T8 bulge is shown in wheat color.

(C) The measured hydrogen bond distances (hetero atom-hetero atom) for the weakened A7-T7' and G8-C8' Watson-Crick pairs flanking the inserted T bulge in the 7T8 bulge-containing *Tt*Ago ternary complex.

(D, E) Comparison of structures of non-bulge control (panel D) and 7T8 bulge-containing (panel E) *Tt*Ago ternary complexes. The Ago is shown in a color-coded surface representation and the DNA guide (red)-DNA target (blue) in a ribbon representation. The PAZ domain cannot be traced in the 7T8 ternary complex.

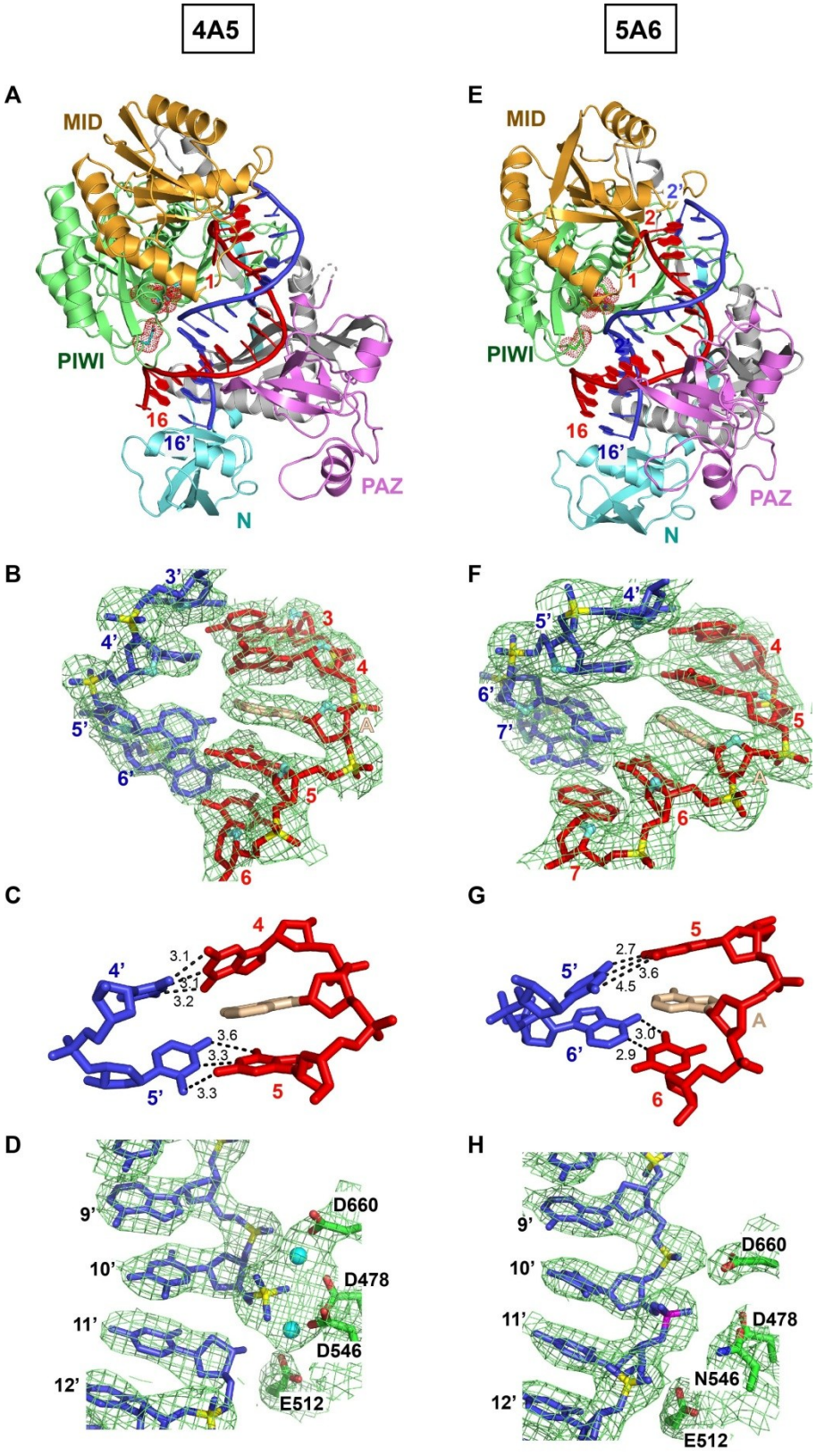

Figure S2. Overall Structures and Details of Stacked-in Adenine in the *Tt*Ago Ternary Complexes Containing a 4A5 Bulge (*Tt*Ago Wild-type) and

5A6 Bulge (*Tt*Ago D546N Catalytic Mutant) Within the Seed Segment of the DNA Guide Strand.

(A) 3.1 Å structure of *Tt*Ago (wild-type) bound to 5'-phosphorylated 22-nt guide DNA (in red) and 19-nt target DNA (in blue) containing a 4A5 bulge positioned on the guide strand within the seed segment.

(B) 2Fo-Fc electron density maps (1σ) for the guide (nts 3-6) and target (nts 3'-6') strands of the 4A5 bulge on the guide strand of the *Tt*Ago (wild-type) ternary complex. The stacked-in A of the 4A5 bulge is shown in wheat color.

(C) The measured hydrogen bond distances (hetero atom-hetero atom) for the weakened G5-C5' Watson-Crick pair flanking the inserted A bulge in the 4A5 bulge-containing *Tt*Ago (wild-type) ternary complex.

(D) 2Fo-Fc electron density maps (1σ) for the target (nts 9'-12') strand and catalytic residues in the 4A5 bulge-containing *Tt*Ago (wild-type) ternary complex. Note the broken phosphodiester linkage at the 10'-11' step and the two bound Mg^{2+} cations.

(E) 2.8 Å structure of *Tt*Ago (N546 catalytic mutant) bound to 5'-phosphorylated 22-nt guide DNA (in red) and 19-nt target DNA (in blue) containing a 5A6 bulge positioned on the guide strand within the seed segment.

(F) 2Fo-Fc electron density maps (1σ) for the guide (nts 4-7) and target (nts 4'-7') strands of the 5A6 bulge on the guide strand of the *Tt*Ago (D546N catalytic mutant) ternary complex. The stacked-in A of the 5A6 bulge is shown in wheat color.

(G) The measured hydrogen bond distances (hetero atom-hetero atom) for the weakened G5-C5' Watson-Crick pair flanking the inserted A bulge in the 5A6 bulge-containing *Tt*Ago (D546N catalytic mutant) ternary complex.

(H) 2Fo-Fc electron density maps (1σ) for the target (nts 9'-12') strand and catalytic residues in the 5A6 bulge-containing *Tt*Ago (D546N catalytic mutant) ternary complex. Note the intact phosphodiester linkage at the 10'-11' step.

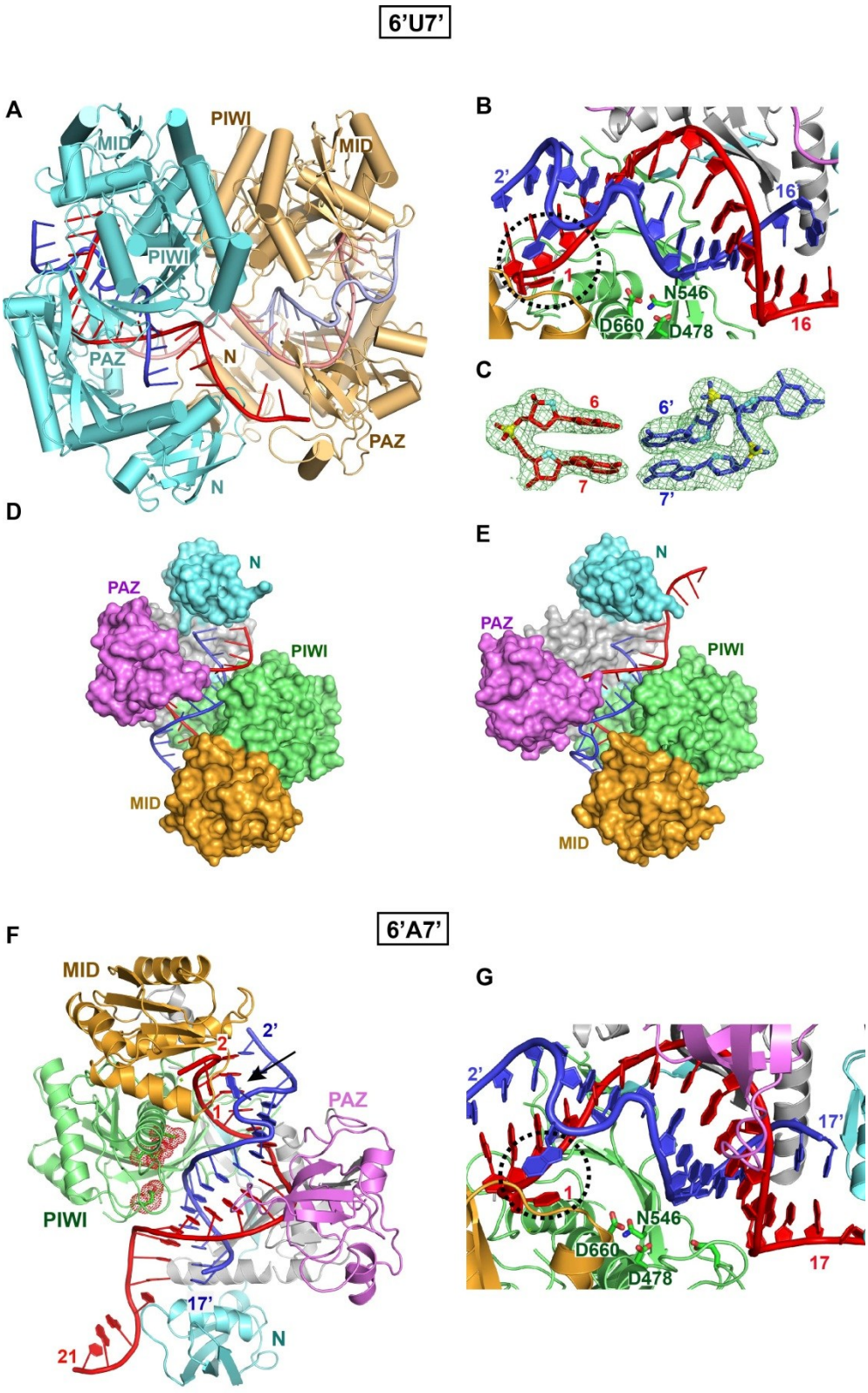

Figure S3. Packing Arrangement in the Crystal Lattice and Details of the Looped- out Base in the *Tt*Ago (D546N Catalytic Mutant) Ternary Complex Containing a 6'U7' and 6'A7' Bulges Within the Seed Segment of the RNA Target Strand.

(A) Packing arrangement of two guide-target duplexes and two Ago molecules in the 2.8 Å structure of the ternary complex of the 6'U7'-containing bulge on the target strand. The 5'-end of the DNA guide is anchored in the Mid domain of one Ago molecule and its 2-nt 3'-end is anchored in the PAZ domain of a second Ago molecule. The guide DNA can be traced for the entire 1-21 segment, while the target RNA can be traced for the 2'-16' segment.

(B) A view of the guide-target duplex in the ternary complex of the 6'U7'-containing bulge on the target strand. Note the stacking of the uracil bulge on the unpaired first base of the guide strand (shown by a dashed circle).

(C) A 2Fo-Fc electron density map contoured at 1.5σ highlighting the bulge site with the looped-out uracil flanked by Watson-Crick A-T and reversed non-canonical A•A pairs in the structure of the ternary complex.

(D, E) Comparison of the structures of non-bulge control (panel D) and 6'U7' bulge-containing (panel E) *Tt*Ago ternary complexes. The Ago is shown in a color-coded surface representation and the DNA guide (red)-RNA target (blue) in a ribbon representation.

(F) 3.2 Å structure of *Tt*Ago (N546 catalytic mutant) bound to 5'-phosphorylated 21-nt guide DNA (in red) and 20-nt target RNA (in blue) containing a 6'A7' bulge positioned on the target strand within the seed segment. The black arrow points to the looped-out bulge base. There is one molecule of the complex in the asymmetric unit and the 3'-end of the guide strand is inserted into the PAZ pocket of an adjacent molecule in the crystal lattice (not shown).

(G) A view of the guide-target duplex in the ternary complex of the 6'A7'-containing bulge on the target strand. Note the stacking of the adenine bulge on the unpaired first base of the guide strand (shown by a dashed circle).

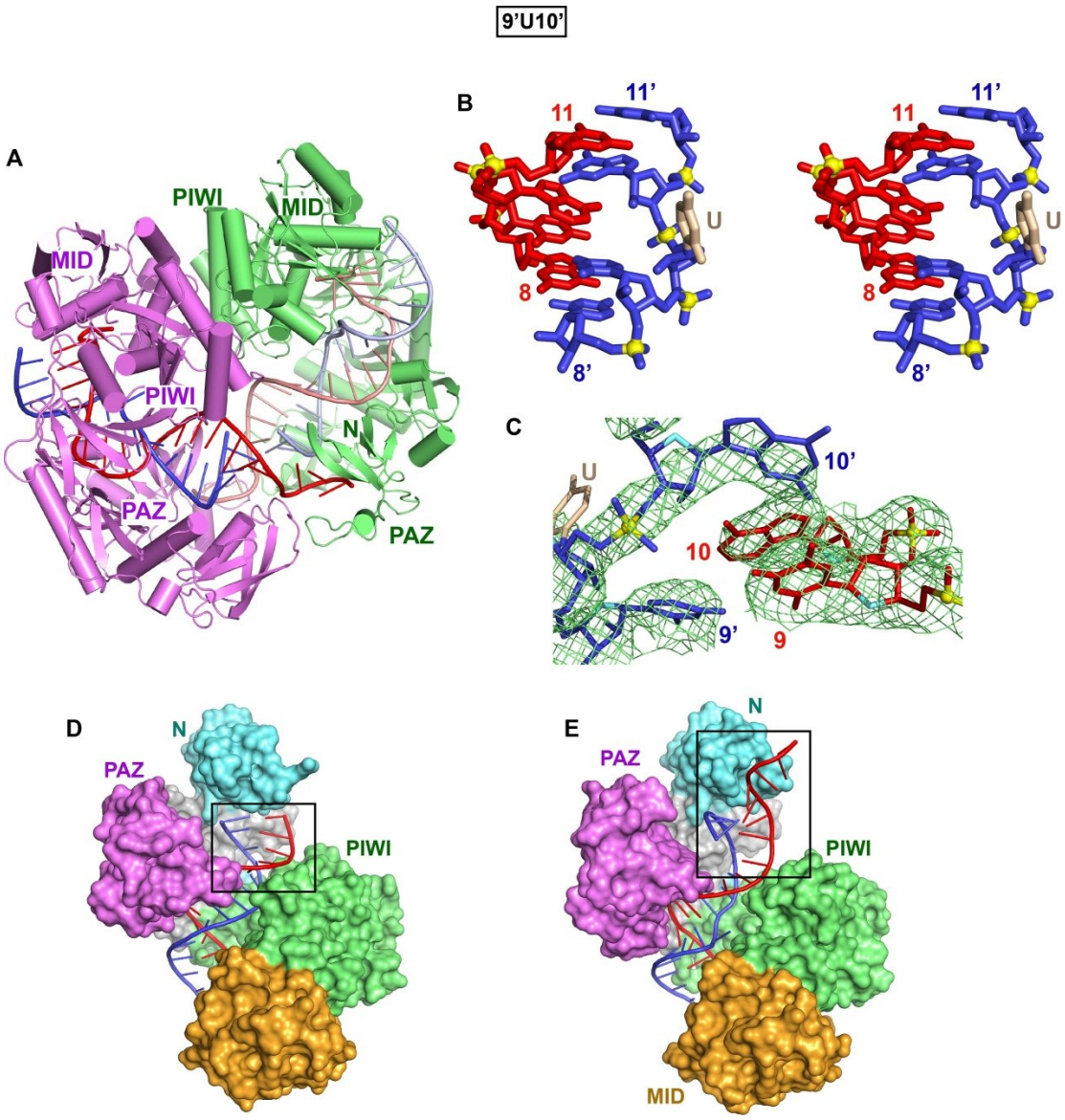

Figure S4. Packing Arrangement in the Crystal Lattice and Details of the Looped- out Uracil in the *Tt*Ago (D546N Catalytic Mutant) Ternary Complex Containing a 9'U10' Bulge Within the Seed Segment of the RNA Target Strand.

(A) Packing arrangement of two guide-target duplexes and two Ago molecules in the 2.9 Å structure of the ternary complex of the 9'U10'-containing bulge on the target strand. Unexpectedly, the 5'-end of the DNA guide is anchored in the Mid domain of one Ago molecule and its 2-nt 3'-end is anchored in the PAZ domain of a second Ago molecule.

(B) A stereo view in stick of the looped out uracil and two flanking base pairs in the structure of the 9'U10' bulge-containing *Tt*Ago ternary complex.

(C) 2Fo-Fc electron density maps (1σ) for the bulged uracil and flanking non-canonical T9•U9' and sheared A10•G10' pairs. We can observe electron density for the sugar but not the base of the bulged uracil.

(D, E) Comparison of structures of non-bulge control (panel D) and 9'U10' bulge-containing (panel E) *Tt*Ago ternary complexes. The boxed segment highlights differences between the two complexes. The Ago is shown in a color-coded surface representation and the DNA guide (red)-RNA target (blue) in a ribbon representation.

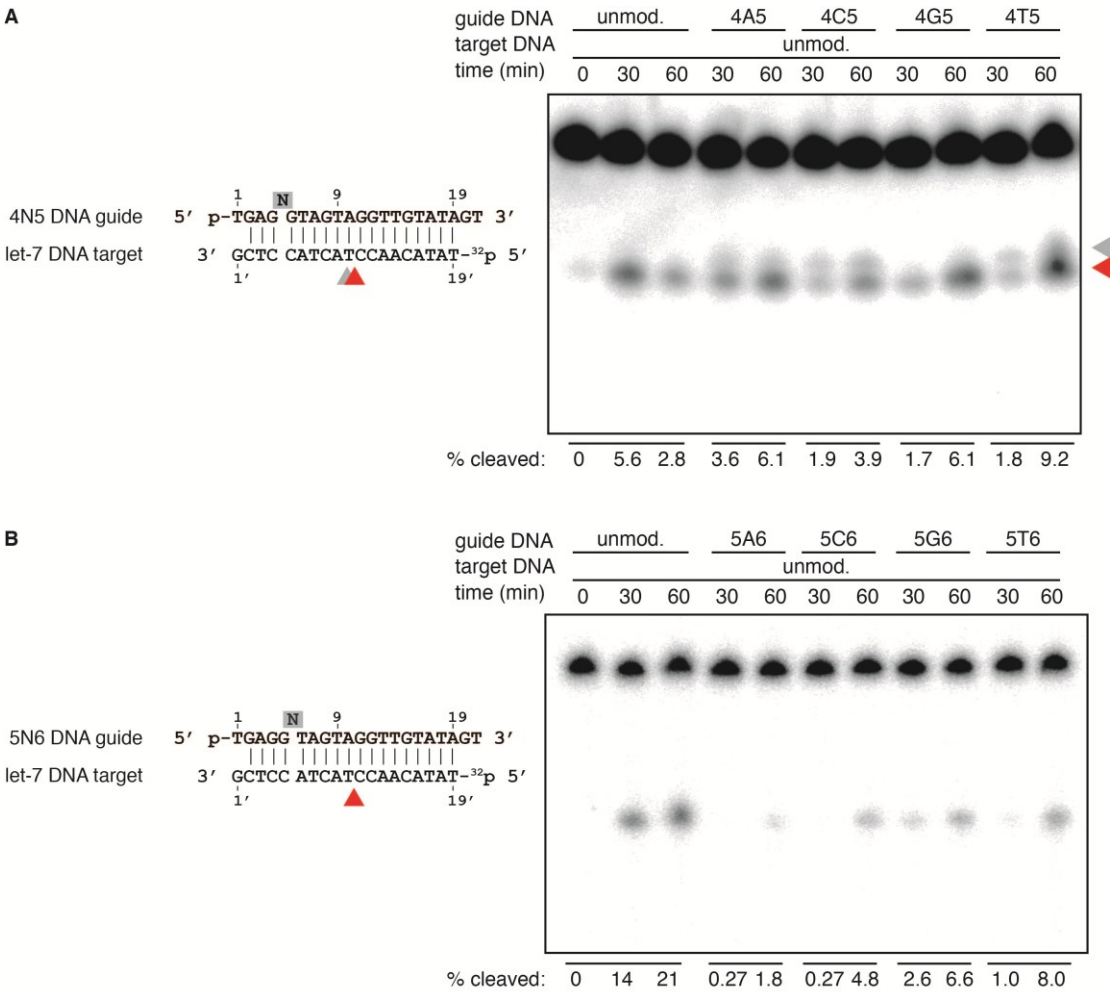

Figure S5. Effect of the Position and Identity of the Inserted Nucleotide in the Guide Strand on DNA Cleavage.

*Tt*Ago was loaded with 5' phosphorylated guide DNAs at 55 °C for 30 min prior to addition of 5' radiolabeled let-7 DNA target, followed by incubation at 75 °C for indicated times. Products were resolved on a 15% denaturing polyacrylamide gel. The fraction of target cleaved was quantified by phosphorimaging and is shown at the bottom. The position of nucleotide insertion is highlighted in gray in each representative guide/target pair. The observed cleavage site is indicated by the red arrowheads.

(A) Bulges 4N5 do not affect cleavage activity but affect accuracy as indicated by the appearance of minor cleavage products indicated by gray arrowheads, regardless of the identity of the inserted nucleotide. Note that lane 3 (60 min) was under-loaded, hence the lower fraction cleaved compared to the earlier time point (30 min).

(B) Bulge 5N6 substantially reduce cleavage activity and minor cleavage products if generated remain undetectable.

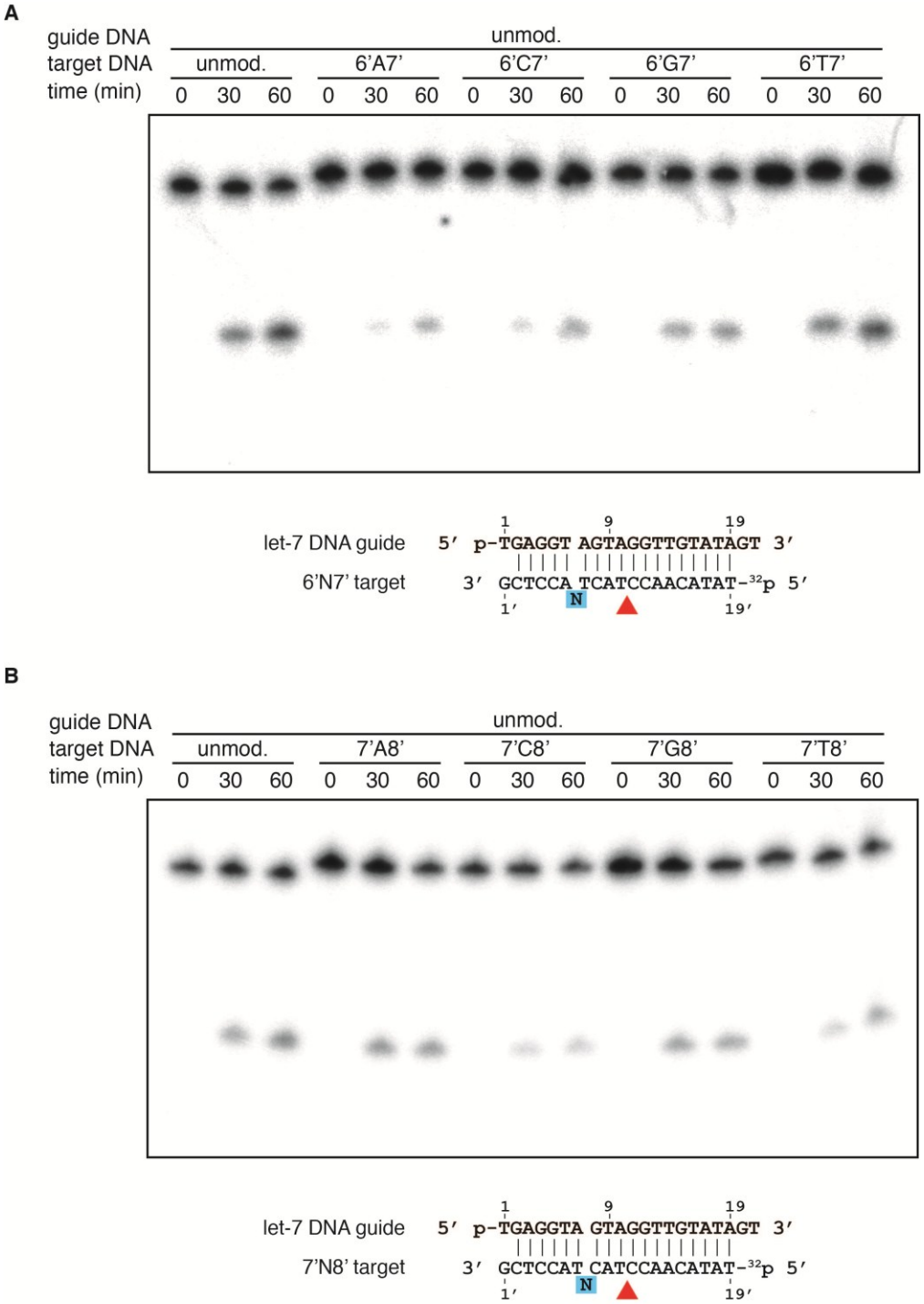

Figure S6. Effect of the Position and Identity of Target Insertions on DNA Cleavage.

(A, B) Similarly to Fig. 6c, the effects of each possible insertion between positions 6' and 7' (A) and 7' and 8' (B) were examined. The position of nucleotide insertion in the target is highlighted in blue in each representative

guide/target pair. Although there are differences in the efficiency of cleavage, all insertions showed cleavage activity at the same position as let-7 target.